Master figs.

Analysis of a wavy crack in sandwich specimens

A.R. Akisanya and N.A. Fleck

Cambridge University Engineering Department,

Trumpington Street, Cambridge CB2 1PZ, England.

Abstract

A crack in a brittle adhesive layer joining two substrates can grow in a variety of ways. The crack can grow along one of the interfaces, within the adhesive or alternate between the two interfaces. In this paper, we consider a crack that grows along an alternating path between the two interfaces. A quantitative analysis of this elastic problem is carried out using the finite element method to predict the wavelength of the alternating crack. The joint is loaded remotely by the singular stress field for a cracked homogeneous solid, parameterised by K_I^∞ and K_{II}^∞, and by an in-plane tensile residual stress σ_o in the layer, parallel to the interface. The induced interfacial stress intensity factor and its phase angle ψ are evaluated and used to predict the onset of kinking out of the interface. The wavelength of the alternating crack is found to depend on the elastic mismatch parameters, α and β, and on the level of residual stress in the layer, parameterised by $\zeta = \frac{\sigma_o\sqrt{h}}{\sqrt{\bar{E}_*\Gamma_I}}$, where h is the adhesive layer thickness, $\bar{E}_*$ is a modulus quantity and Γ_I is the toughness of the interface.

1 Introduction

Adhesive joints are increasingly used for structural applications in aerospace, automotive and in general engineering. The adhesive layer may be metallic (brazed and soldered joints), polymeric (for example epoxy or cyanoacrylate), or ceramic (such as glass). Joints contain flaws; the observed strength of the joint is dependent upon the location of the flaws and the crack path through the joint. Recent work, e.g. Zdaniewski [1], Chai [2, 3, 4], Cao and Evans [5], Wang and Suo [6] and Dalgleish et al. [7, 8] on characterization of the interfacial fracture resistance have shown that cracks in the adhesive layer between two substrates grow in a variety of ways. The crack may grow along one of the interfaces, within the adhesive, alternate between the adhesive and an adjacent material or alternate between the two interfaces. The experimentally measured toughness and therefore the strength of the joint depend on the actual path adopted by the crack. For example, the observed toughness is that of the interface when the crack grows along either of the interfaces and that of the adjacent material when the crack tip lies in that material.

In this paper we consider an interfacial crack which grows by kinking periodically from one interface to the other across an adhesive layer. This cracking mode has been observed by Chai [4] for an epoxy layer sandwiched between two aluminium adherends, see Figure 1. He used a double cantilever beam (DCB) specimen geometry, loaded in mode I. The aim of the present work is to predict this alternating crack trajectory.

The idealised geometry is shown in Figure 2. We replace the specimen by a circular domain of radius R, loaded remotely by the crack tip stress intensity factor $\mathbf{K}^{\infty} = K_I^{\infty} + iK_{II}^{\infty}$ for the homogeneous base specimen neglecting the presence of the layer. Here, $\mathbf{K}^{\infty}$ is written as a complex number and $i = \sqrt{-1}$. $\mathbf{K}^{\infty}$ is related to the remotely applied loads and the particular specimen geometry as cataloged for example by Tada et al. [9]. Loading is achieved by imposing the asymptotic crack tip stress field for a homogeneous body as a traction condition on the circular boundary of the idealised geometry. A residual tensile stress σ_o also exists in the

adhesive layer of thickness h, as shown in Figure 2. The residual tensile stress σ_o in the layer is represented by a normal traction of magnitude σ_o across the kinked segment of the crack, as shown in Figure 2. We assume that an interfacial crack has advanced by a length ℓ from the previous kink, and explore the necessary and sufficient conditions for this interfacial crack to kink into the adhesive layer. After the crack kinks we expect it to grow across the adhesive layer (driven largely by the tensile residual stress σ_o), impinge upon the opposite interface and become a new interfacial crack. This crack advances until it attains the critical length and kinks back into the adhesive layer, and the cycle is repeated.

We focus attention on an interfacial crack of length ℓ from the previous kink, as shown in Figure 2. The complex interfacial stress intensity factor $\mathbf{K}$ is defined such that at a distance r ahead of the crack tip, the normal stress σ_{yy} and shear stress σ_{xy} components are given by,

$$\sigma_{yy} + i\sigma_{xy} = \frac{1}{\sqrt{2\pi}}\mathbf{K}r^{-1/2+i\varepsilon} \tag{1}$$

Here, the material parameters α, β and ε measure the elastic mismatch between the adhesive material 2 and the adherend material 1, and are defined for plane strain conditions by [10]

$$\begin{aligned} \alpha &= \frac{(1-\nu_2)/\mu_2 - (1-\nu_1)/\mu_1}{(1-\nu_2)/\mu_2 + (1-\nu_1)/\mu_1} \\ \beta &= \frac{1}{2}\frac{(1-2\nu_2)/\mu_2 - (1-2\nu_1)/\mu_1}{(1-\nu_2)/\mu_2 + (1-\nu_1)/\mu_1} \\ \varepsilon &= \frac{1}{2\pi}\ln\frac{1-\beta}{1+\beta} \end{aligned} \tag{2}$$

where ν and μ are the Poisson's ratio and the shear modulus respectively.

The remote stress intensity factor $\mathbf{K}^\infty$ has the dimension

$$\mathbf{K}^\infty \sim (stress)\sqrt{\ell} \tag{3}$$

The interfacial stress intensity factor $\mathbf{K}$ has the dimension

$$\mathbf{K} \sim (stress)h^{1/2-i\varepsilon} \tag{4}$$

where we choose the adhesive layer thickness h to be the characteristic length in the definition of $\mathbf{K}$.

Dimensional considerations dictate that the interfacial stress intensity factor $\mathbf{K}$ is related to the residual tensile stress σ_o in the layer, and the remote stress intensity factor $\mathbf{K}^\infty = K_I^\infty + iK_{II}^\infty$ by

$$\mathbf{K}h^{i\varepsilon} = a\mathbf{K}^\infty + \bar{b}\bar{\mathbf{K}}^\infty + e\sigma_o\sqrt{h} \tag{5}$$

Here, a, b and e are non-dimensional complex functions of α, β and ℓ/h, and $(^-)$ denotes the complex conjugate. Specific determination of the non-dimensional functions a, b and e requires that the crack problem be solved for three loading cases for a given α, β and ℓ/h. This has been done using a finite element procedure. The details of the solution procedure are given in section 3.

The elastic strain energy release rate G_I for the interfacial crack as it grows away from the previous kink is given by

$$\bar{E}_* G_I = \mid \mathbf{K} \mid^2 = \mid \mathbf{K}h^{i\varepsilon} \mid^2 \tag{6}$$

where [11]

$$\frac{1}{\bar{E}_*} = \frac{1}{2}\left[\frac{1}{\bar{E}_1} + \frac{1}{\bar{E}_2}\right]\frac{1}{Cosh^2(\pi\varepsilon)} \tag{7}$$

and $\bar{E} = E/(1-\nu^2)$ is the plane strain tensile modulus. By substituting for $\mathbf{K}h^{i\varepsilon}$ from equation (5) in equation (6), G_I can be expressed in the form

$$\frac{\bar{E}_* G_I}{\sigma_o^2 h} = \frac{f_1 + \eta f_2 + \eta^2 f_3}{\eta^2} \tag{8}$$

where

$$\begin{aligned}
\eta &= \sigma_o\sqrt{h}/K_I^\infty \\
f_1 &= \left[\mid a \mid^2 + \mid b \mid^2 + 2Re(abe^{2i\phi})\right]\left[1 + (K_{II}^\infty/K_I^\infty)^2\right] \\
f_2 &= 2Re\left[e(be^{i\phi} + \bar{a}e^{-i\phi})\right]\left[1 + (K_{II}^\infty/K_I^\infty)^2\right]^{1/2} \\
f_3 &= e_R^2 + e_I^2 \\
\phi &= \arctan(K_{II}^\infty/K_I^\infty)
\end{aligned} \tag{9}$$

Consider an interfacial crack with a pre-existing kink of length s at an orientation ω to the interface. A necessary condition for the interfacial crack to kink out of the interface is that the stress intensity factors at the tip of the kink suffer the condition

$K_{II} \geq 0$, $K_I > 0$. A kinked crack with $K_{II} < 0$ is driven upward back to the interface. The stress intensity factors K_I and K_{II} at the tip of a kink depend upon the orientation ω of the kink, the normalised kink length s/h, the elastic mismatch parameters α, β and upon the phase angle ψ of the interfacial crack, where

$$\psi = \arctan\left[\frac{Im(\mathbf{K}h^{i\varepsilon})}{Re(\mathbf{K}h^{i\varepsilon})}\right] \tag{10}$$

We argue that the alternating crack trajectory [4] is due to kinking of the interfacial crack from flaws at an angle $\omega = 0$ to the interface. Examination of the alternating crack trajectory reported by Chai [4] (see Figure 1) reveals that the interfacial crack leaves the interface along a trajectory of continuous slope. Also, the substrates were polished and etched prior to bonding. **We deduce that flaws exist predominantly at $\omega = 0$ in Chai's specimens.**

The phase angle ψ of the interfacial crack shown in Figure 2 is a function of the remote loading parameter $\sigma_o\sqrt{h}/\mid \mathbf{K}^\infty \mid$, phase angle of remote loading $\phi = \arctan(K_{II}^\infty/K_I^\infty)$, geometry ℓ/h and of the material parameters α and β. As the interfacial crack of length ℓ grows away from the previous kink (see Figure 2), the phase angle ψ increases.

Kinking of the main crack out of the interface occurs when the stress intensity factors at the tip of a pre-existing kink (at $\omega = 0$) satisfy the condition $K_{II} \geq 0$, $K_I > 0$. The He and Hutchinson [12] analysis gives the corresponding critical interfacial phase angle ψ_c. The critical phase angle ψ_c is a function of α, β and s/h (see Figure 5) where s is the assumed length of a pre-existing flaw at the tip of the interfacial crack. For example, for an aluminium/epoxy system α equals 0.93, β equals 0.22 and ψ_c equals -45^o assuming s/h equals 0.01. We shall show that the interfacial crack extends until a length ℓ_c when $\psi = \psi_c$, and kinking occurs. When the interfacial crack kinks it leaves the interface and grows along a path of continuous slope into the adhesive.

The outline of this paper is as follows. First, we consider the implications of the He and Hutchinson [12] analysis for kinking of the interfacial crack shown in Figure 2. The interfacial stress intensity factor $\mathbf{K}$ is calculated as a function of remote loading σ_o and $\mathbf{K}^\infty$, using a finite element procedure. The critical crack length ℓ_c at

which kinking occurs is deduced. Finally, the conditions are described for which an alternating crack trajectory is expected.

2 Kinking analysis

He and Hutchinson [12] have recently proposed a model for predicting the kinking of a semi-infinite interfacial crack out of the interface. They consider an interfacial crack between two isotropic materials 1 and 2, loaded by the interfacial stress intensity factor $\mathbf{K}$, as shown in Figure 3. A kink-like flaw of length s at angle ω to the interface extends from the crack tip into material 2, see Figure 3. The stress intensity factor at the kink tip is given by [12]

$$K_I + iK_{II} = c\mathbf{K}s^{i\varepsilon} + d\bar{\mathbf{K}}s^{-i\varepsilon} \tag{11}$$

where the non-dimensional complex functions c, d depend upon ω, α and β, and have been given explicitly by He and Hutchinson [13]. The strain energy release rate for the kink crack G_S is related to the strain energy release rate for the interfacial crack G_I by [12]

$$\frac{G_S}{G_I} = \left(\frac{1+\alpha}{1-\beta^2}\right)\left[\mid c \mid^2 + \mid d \mid^2 + 2Re(cde^{2i\bar{\psi}})\right] \tag{12}$$

where the phase angle $\bar{\psi}$ is given by

$$\bar{\psi} = \arctan\left[\frac{Im(\mathbf{K}s^{i\varepsilon})}{Re(\mathbf{K}s^{i\varepsilon})}\right] \tag{13}$$

The phase angle ψ defined in equation (10) is related to $\bar{\psi}$ by

$$\psi = \arctan\left[\frac{Im(\mathbf{K}h^{i\varepsilon})}{Re(\mathbf{K}h^{i\varepsilon})}\right] = \bar{\psi} - \varepsilon \ln(s/h) \tag{14}$$

We assume that flaws to initiate kinking exist only at $\omega = 0$, which is consistent with experimental observations of Chai [4] for the alternating crack trajectory. The dependence of K_I and K_{II} at the kink tip on phase angle $\bar{\psi} < 0$, and on kink angle ω is shown in Figure 4 for $\alpha = 0.8$, $\beta = 0$ and for $\alpha = 0.8$, $\beta = 0.2$.

Consider the conditions at the tip of a flaw orientated at a vanishingly small angle to the interface $\omega = 0$, for $\alpha = 0.8$ and $\beta = 0.2$, see Figure 4b. We assume that the

toughness of the substrate material 1 greatly exceeds that of the adhesive material 2 and the interfacial toughness. For $\bar{\psi}$ in the range of $-90° < \bar{\psi} < -20°$, we find that K_{II} is negative and K_I is positive: the crack remains in the interface. When $\bar{\psi}$ attains a critical value $\bar{\psi}_c = -20°$ for this material combination the flaw orientated at $\omega = 0$ suffers $K_{II} = 0$ and $K_I > 0$; the flaw propagates into the adhesive material at a vanishingly small initial angle to the interface. When $\bar{\psi}$ exceeds $\bar{\psi}_c$, we find $K_{II} > 0$ and $K_I > 0$, and the flaw kinks down into the adhesive material 2 at a finite positive angle.

Now consider the case $\alpha = 0.8$, $\beta = 0$. The critical phase angle $\bar{\psi}_c$ at which a flaw orientated at $\omega = 0$ grows in a self similar manner is now $\bar{\psi}_c = -5°$. Otherwise, the behaviour is qualitatively the same as for $\alpha = 0.8$, $\beta = 0.2$.

The critical phase angle $\bar{\psi}_c$ depends only on the elastic mismatch parameters α and β. It decreases with increasing α and β, as shown in Figure 5.

He and Hutchinson [12] have shown that for a fixed $\bar{\psi}$ the kink orientation ω satisfying the condition $K_{II} = 0$ at the kink tip differs by less than 1° from the orientation ω for which $G_S(\alpha, \beta, \bar{\psi}, \omega)$ is a maximum. For a flaw at $\omega = 0$, equation (12) yields $G_S/G_I = 1.0$ to 1.1 for $\bar{\psi} = \bar{\psi}_c$, and α, β in the range $0.5 < \alpha < 1$, $0 < \beta < 0.25$.

For the problem of the alternating crack trajectory, we shall show that the interfacial crack of length ℓ from the previous kink (Figure 2) suffers the condition $\bar{\psi} < \bar{\psi}_c$ at small ℓ/h and $\bar{\psi} > \bar{\psi}_c$ at large ℓ/h. The wavelength of the crack trajectory is set by the onset of growth into the adhesive material at a value of ℓ/h corresponding to $\bar{\psi} = \bar{\psi}_c$.

So far we have discussed the necessary condition for crack kinking. Kinking will only occur if sufficient energy is available to drive the kink. Thus the sufficient condition for kinking is [12]

$$\frac{\Gamma_I(\bar{\psi})}{\Gamma_S} \geq \frac{G_I}{G_S^*} \tag{15}$$

where Γ_S is the toughness of material 2 into which the crack kinks and Γ_I is the toughness of the interface for a phase angle $\bar{\psi}$. G_S^* is the energy release rate along the kink orientation ω satisfying the condition $K_{II} = 0$ at the kink tip. For the

problem of the alternating crack trajectory, Chai [3, 4], we find the inequality in equation (15) is satisfied upon substituting measured material properties into the equation.

3 Numerical Analysis

The interfacial crack shown on Figure 2 suffers mixed-mode loading, even when the remote load is mode I. A method to evaluate the stress intensity factors in a mixed-mode problem is to consider the interaction energy between the elastic state of interest and an auxiliary state. By choosing an appropriate auxiliary state, the stress intensity factors can be computed through an associated path-independent integral. The general concept is given by Chen and Shield [14].

Recently, Matos et al. [15] used Parks' [16] virtual crack extension technique in conjunction with this method to evaluate the J-integral for an interfacial crack. This method is adopted in the present analysis to evaluate the interfacial stress intensity factor.

The remote load on the circular boundary of the idealised geometry is taken as the singular crack tip stress field for a crack in a homogeneous material with stress intensity factors K_I^∞ and K_{II}^∞. The residual tensile stress σ_o in the layer is represented by a normal traction of magnitude σ_o across the kinked segment of the crack. The auxiliary field is the singular crack tip displacement field for an interfacial crack.

An elastic analysis was carried using the finite element code MARC-K3 [1]. The finite element mesh is shown in Figure 6. The mesh contains 2460 elements with 40 crack tip elements, each of size 0.03h. The elements are eight-noded plane strain isoparametric quadrilateral with 3x3 gauss points of integration. The square root singularity is modelled by moving the mid-side nodes on the side adjacent to the crack tip to the quarter point position for all crack tip elements. The displacements, connectivities and coordinates for all the elements within the ring to be deformed

[1]MARC-CDC (1974), MARC Analysis Research Corp., Providence, R.I.

during virtual crack extension were written to an output file and later used to evaluate the stress intensity factors using the method of Matos et al. [15].

The coefficients a, b and e in equation (5) were determined by applying the three independent loads K_I^∞, K_{II}^∞ and σ_o in turn. Results are given in Appendix A for a variety of material combinations and crack lengths. Mesh convergence studies suggest that the results are accurate to within 1 %.

4 Results and Discussion

Most material combinations have small values of β, ($\beta << 1$), (Hutchinson et al. [17]), and thus the assumption that $\beta = 0$ can sometimes be made. Moreover, data for typical material combinations are concentrated along the line $\beta = \alpha/4$ in $\alpha - \beta$ space [18]. This corresponds to $\nu_1 = \nu_2 = 1/3$. Here, discussion is restricted to material combinations with $\beta = 0$ and those with $\beta = \alpha/4$. Also, we consider the case of remote mode I loading, since the alternating crack trajectory is observed for a mode I specimen geometry.

4.1 Effect of remote load

The components of the interfacial stress intensity factor are deduced from equation (5) as,

$$Re(\mathbf{K}h^{i\varepsilon}) = (a_R + b_R)K_I^\infty - (a_I + b_I)K_{II}^\infty + e_R\sigma_o\sqrt{h} \tag{16}$$

$$Im(\mathbf{K}h^{i\varepsilon}) = (a_I - b_I)K_I^\infty + (a_R - b_R)K_{II}^\infty + e_I\sigma_o\sqrt{h}$$

and the phase angle ψ is

$$\psi = \arctan\frac{Im(\mathbf{K}h^{i\varepsilon})}{Re(\mathbf{K}h^{i\varepsilon})} = \arctan\frac{(a_I - b_I) + (a_R - b_R)K_{II}^\infty/K_I^\infty + e_I\sigma_o\sqrt{h}/K_I^\infty}{(a_R + b_R) - (a_I + b_I)K_{II}^\infty/K_I^\infty + e_R\sigma_o\sqrt{h}/K_I^\infty} \tag{17}$$

For a base specimen under a remote mode I load ($K_{II}^\infty/K_I^\infty = 0$), and with no residual stress in the layer, the variation of the interfacial stress intensity factor with crack length is shown in Figure 7a for $\alpha = 0.80$, ($\beta = 0$ and $\alpha/4$). For both values of β, the real component, $Re(\mathbf{K}h^{i\varepsilon})$, is always greater that the imaginary

component, $Im(\mathbf{K}h^{ie})$. The stress intensity factor attains a steady-state condition when $\ell/h \geq 2$. The effect of β on the stress intensity factor is negligible.

4.2 Effect of residual stress

The variation of the induced interfacial stress intensity factor due to in-layer tensile residual stress σ_o with crack length is shown in Figure 7b. The real and the imaginary parts are both negative, decreasing (i.e. becoming more negative) initially and later increasing with crack length. They both exhibit minima in the region $\ell/h \approx 0.50$ and asymptote to zero for a crack tip far from its previous kink, since there is no energy release rate due to residual stress for a semi-infinite interfacial crack. The effect of β on both the real and imaginary parts is negligible.

An asymptotic expression is derived in Appendix B for the stress intensity factor due to the residual stress when the interfacial crack is long compared with the adhesive layer thickness.

4.3 Coupled effect of remote and residual stresses

In practice, crack growth in adhesively bonded joints is driven by both remote and residual stresses. The dependence of the phase angle ψ on the crack length, and $\sigma_o\sqrt{h}/K_I^\infty$ is shown in Figure 8. For a given value of $\sigma_o\sqrt{h}/K_I^\infty$, ψ approaches the steady state phase angle ψ_{SS} as the crack length increases.

4.4 Prediction of alternating crack trajectory

The steady state phase angle ψ_{SS} of a semi-infinite crack at the upper interface of a sandwich specimen loaded as shown in Figure 9 is given by [19]

$$\psi_{SS} = \Omega(\alpha, \beta) + \phi \tag{18}$$

where $\Omega(\alpha, \beta)$ is the shift in phase angle tabulated in [19] and $\phi = \arctan(K_{II}^\infty/K_I^\infty)$. Figure 5 shows the dependence of ψ_{SS} on α and β when $K_{II}^\infty = 0$.

As the interfacial crack of length ℓ grows away from the previous kink its phase angle ψ increases to the steady state value ψ_{SS}, see Figure 8. The interfacial energy

release rate at this stage of growth equals the interfacial toughness at the relevant phase angle. We assume that the crack leaves the interface when $\psi = \psi_c$, where ψ_c is related to $\bar{\psi}_c$ via equation (14). Note that ψ_c depends upon (α, β) and upon s/h for $\varepsilon \neq 0$ (i.e. $\beta \neq 0$), where s is the length of pre-existing interfacial flaws with orientation $\omega = 0$. The dependence of ψ_c on α, β and s/h is included in Figure 5. When ψ_c is less than ψ_{SS}, the interfacial phase angle ψ attains the value ψ_c first and it is possible for the crack to leave the interface. But when ψ_c is greater than ψ_{SS}, ψ never attains the value ψ_c and the crack remains in the interface. We note that ψ_c is less than ψ_{SS} for $\beta = \alpha/4$ (Figure 5), and kinking is possible. ψ_c is greater than ψ_{SS} for $\beta = 0$ and kinking is not predicted.

The steady state phase angle ψ_{SS} is a function of α, β and the phase angle of the remote load, $\phi = \arctan(K_{II}^{\infty}/K_I^{\infty})$, while the critical phase angle ψ_c depends upon α, β and s/h. In the present study we assume remote mode I loading with $K_{II}^{\infty}/K_I^{\infty} = 0$. We find that the alternating crack trajectory is expected for (α, β) values occupying a region of (α, β) space. This is shown in Figure 10 for the case $s/h = 0.01$. We conclude that the kinking phenomenon requires $\beta > 0.06\alpha$ for $s/h = 0.01$.

The critical crack length ℓ_c at which the interfacial crack kinks across the adhesive layer may be calculated as follows. Consider the geometry shown in Figure 2 and assume given values of α, β and s/h. Kinking out of the interface begins when $\psi(\sigma_o\sqrt{h}/K_I^{\infty}, \ell/h, \alpha, \beta) = \psi_c(s/h, \alpha, \beta)$. ψ is given as a function of $\sigma_o\sqrt{h}/K_I^{\infty}$, ℓ/h, α and β in equation (17), and ψ_c is shown in Figure 5. We use the equality $\psi = \psi_c$ in equation (17) in order to deduce $\sigma_o\sqrt{h}/K_I^{\infty}$ as a funtion of ℓ/h, for the chosen values of α, β and s/h. The corresponding normalised energy release rate $\bar{E}_* G_I/\sigma_o^2 h$ is evaluated from equation (8). Recalling that $G_I = \Gamma_I(\psi_c)$ and $\ell = \ell_c$ for the critical interfacial crack at the initiation of kinking, we plot ℓ_c/h versus $\zeta = (\bar{E}_* \Gamma_I(\psi_c)/\sigma_o^2 h)^{-1/2}$ in Figure 11.

We note from Figure 11 that the critical length ℓ_c/h increases with ζ. A low value of $\Gamma_I(\psi_c)$ implies that the crack remains in the interface over a longer increment ℓ_c, as expected. The effect of an increased value of σ_o is to make ψ more negative for a

given value of ℓ, and hence delay kinking. This contradicts a simple but erroneous energy argument that ℓ_c decreases with increasing σ_o in order to maximise the release of stored elastic strain energy.

Once kinking out of the upper interface has occurred, the strain energy release rate of the crack in the adhesive layer increases with crack extension: the crack is driven by tensile residual stress σ_o in the layer [20]. Then, the crack is deflected to the lower interface and becomes a new interfacial crack along the lower interface. The crack does not advance into the substrate material since it is relatively tough. The process is repeated resulting in an alternating crack path between the interfaces.

5 Case study

Chai [3, 4] has observed the alternating crack trajectory in his test of a double cantilever beam sandwich specimen of an epoxy layer between aluminium substrates. The elastic mismatch parameters for the specimen are $\alpha = 0.93$, and $\beta = 0.22$, which for a specimen under a remote mode I load falls in the region of possible alternating crack trajectory of Figure 10. The epoxy, Narmco 5208, has a toughness $\Gamma_S = 70 - 80 Jm^{-2}$. The thickness of the adhesive layer is $h = 0.25mm$, and the residual stress in the layer σ_o is estimated to be 60 MPa.

In order to predict the wavelength of the alternating crack trajectory using the above theory we need to estimate a value for the interfacial toughness Γ_I at the critical phase angle $\psi_c(\alpha, \beta, s/h)$. Consider interfacial flaws of length s/h = 0.1, 0.01 and 0.001. For the given α, β values, the corresponding values for ψ_c are -34^o, -45^o and -55^o. Unfortunately, the $\Gamma_I(\psi)$ response is not given by Chai. Chai [3] reports a value for Γ_I for interfacial failure in a DCB aluminium/epoxy sandwich specimen of $48 Jm^{-2}$; the steady state interfacial phase angle in this test is $\psi = -13^o$ from Suo and Hutchinson [19]. Examination of the $\Gamma_I(\psi)$ curves for glass/epoxy reported by Liechti and Chai [21] reveals that Γ_I increases by factors of approximately 2, 4 and 6 when ψ is decreased from -13^o to the values -34^o, -45^o and -55^o respectively. As a first guess, we apply these factors to the toughness value $\Gamma_I(\psi = -13^o)$ measured by

Chai [3], and thereby estimate $\Gamma_I(\psi = -34^o) = 90Jm^{-2}$, $\Gamma_I(\psi = -45^o) = 180Jm^{-2}$ and $\Gamma_I(\psi = -55^o) = 270Jm^{-2}$. Substitution of the above values for Γ_I, σ_o, h and the elastic constants into the definition of $\zeta = \sigma_o\sqrt{h}/\sqrt{\bar{E}_*\Gamma_I}$ gives $\zeta = 1.21$, 0.83 and 0.70 for $s/h = 0.1$, 0.01 and 0.001 respectively. Interpolation of the results presented in Figure 11 yields $\ell_c/h = 2.60$, 1.4 and 0.50 for s/h = 0.1, 0.01 and 0.001 respectively. Examination of the fracture surfaces published by Chai [4] reveals $\ell_c/h = 2.8$. This suggests that flaws of length $s = 0.1h = 25\mu m$ exist along the interface, which is reasonable.

6 Concluding discussion.

We conclude that the alternating crack trajectory under remote mode I loading can occur when the following conditions are met:

1. A tensile residual stress exists in the compliant adhesive layer.

2. Interfacial flaws exist at a vanishingly small orientation $\omega = 0$ to the interface. This is achieved by polishing the substrates prior to application of the adhesive.

3. The non-dimensional group $\zeta = \sigma_o\sqrt{h}/\sqrt{\bar{E}_*\Gamma_I}$ lies within a range of values dependent upon α, β and s/h. When s/h = 0.001 - 0.1, ζ must lie in the range $0.1 < \zeta < 2$ for $\alpha = 0.5$, $\beta = \alpha/4$ and in the range $0.5 < \zeta < 12$ for $\alpha = 0.99$, $\beta = \alpha/4$. The upper limit varies somewhat with s/h. The normalised half wavelength ℓ_c/h of the alternating crack trajectory depends upon ζ, s/h, α and β.

He et al. [20] have shown that kinking out of an interface is significantly influenced by in-plane stress parallel to the interface, when the flaw orientation ω is finite. When the substrates of a sandwich specimen have been polished, the interfacial flaws between the substrate and the adhesive are mostly aligned with the interface at an angle $\omega = 0$, and in-plane stresses have no effect upon kinking.

Acknowledgements

The authors are grateful for several helpful discussions with Prof. J.W. Hutchinson, and for unpublished results on crack kinking by Ming He.

References

[1] W.A. Zdaniewski, J.C. Conway and J.P. Kirchner, *Journal of American Ceramic Society* 70 (1987) 110-118.

[2] H. Chai, *Composites* 15 (1984) 277-290.

[3] H. Chai, *Engineering Fracture Mechanics* 24 (1986) 413-431.

[4] H. Chai, *International Journal of Fracture* 32 (1987) 211-213.

[5] H.C. Cao and A.G. Evans, *Mechanics of Materials* 7 (1989) 295-304.

[6] J.S. Wang and Z. Suo, *Acta Metallurgica* 7 (1990) 1279-1290

[7] B.J. Dalgleish, M.C. Lu and A.G. Evans, *Acta Metallurgica* 38 (1988) 2029-2035.

[8] B.J. Dalgleish, K.P. Trumble and A.G. Evans, *Acta Metallurgica* 37 (1989) 1923-1931.

[9] H. Tada, P.C. Paris and G.R. Irwin, *Stress Analysis of Cracks Handbook*, Del Research, St. Louis, MO (1985).

[10] J. Dundurs, in *Mathematical Theory of Dislocations*, American Society of Mechanical Engineering, New York (1969) 70-115.

[11] B.M. Malyshev and R.L. Salgnik, *International of Fracture Mechanics* 1 (1965) 114-128.

[12] M.Y. He and J.W. Hutchinson, *Journal of Applied Mechanics* 56 (1989) 270-278.

[13] M.Y. He and J.W. Hutchinson, Kinking of a crack out of an interface: Tabulated solution coefficients, Havard Univerity Report, MECH-113A, Division of Applied Sciences, Havard University, Cambridge, MA 02138 (1988).

[14] F.J.K. Chen and R.T. Shield, *Journal of Applied Mathematics* 28 (1977) 1-22.

[15] P.P.L. Matos, R.M. McMeeking, P.G. Charalambides and M.D. Drory, *International Journal of Fracture* 40 (1989) 235-254.

[16] D.M. Parks, *International Journal of Fracture Machanics* 10 (1974) 487-502.

[17] J.W. Hutchinson, M.E. Mear and J.R. Rice, *Journal of Applied Mechanics* 54 (1987) 828-832.

[18] T. Suga, G. Elssner and S. Schmander, *Journal of Composite Materials* 22 (1988) 917-934.

[19] Z. Suo and J.W. Hutchinson, *Materials Science and Engineering* A107 (1989) 135-143.

[20] M.Y. He, A. Bartlett, A.G. Evans and J.W. Hutchinson, Kinking of a crack out of an interface; role of in-plane stress, (1990) to be published.

[21] K.M. Liechti and Y.S. Chai, Asymmetric shielding in interfacial fracture under in-plane shear, Engineering Mechanics Research Laboratory, EMRL Report No. 89/4, Department of Aerospace Engineering and Engineering Mechanics, The University of Texas at Austin, Austin, Texas 78712 (1990) to appear in *Journal of Applied Mechanics.*

Appendix A

Tabulated solution coefficients

$\alpha = 0.50, \beta = 0.0$

l/h	a_r	a_i	b_r	b_i	e_r	e_i
0.2	0.3535	0.0912	0.1374	0.2552	-0.1689	-0.5358
0.5	-0.4395	0.0071	0.1206	0.1645	-0.3089	-0.6970
1.0	0.5583	-0.0537	0.0774	0.0712	-0.2544	-0.6813
3.0	0.6665	-0.0774	0.0106	0.0045	-0.0871	-0.3878
6.0	0.6665	-0.0791	-0.0023	-0.0011	-0.0358	-0.2644
10.0	0.6678	-0.0809	-0.0036	-0.0016	-0.0240	-0.2223

$\alpha = 0.80, \beta = 0.0$

l/h	a_r	a_i	b_r	b_i	e_r	e_i
0.2	0.2146	0.0393	0.0977	0.2037	-0.2837	-0.4444
0.5	0.2902	-0.0293	0.0910	0.1261	-0.4399	-0.6391
1.0	0.3751	-0.0865	0.0406	0.0598	-0.3669	-0.6275
3.0	0.4522	-0.1078	-0.0088	0.0019	-0.1261	-0.2955
6.0	0.4589	-0.1115	-0.0138	-0.0048	-0.0481	-0.1735
10.0	0.4593	-0.1117	-0.0141	-0.0053	-0.0340	-0.1447

$\alpha = 0.50, \beta = \alpha/4$

l/h	a_r	a_i	b_r	b_i	e_r	e_i
0.2	0.4005	0.0883	0.1262	0.2585	-0.1187	-0.5791
0.5	0.4939	0.0152	0.1303	0.1547	-0.2633	-0.7073
1.0	0.6054	-0.0481	0.0881	0.0543	-0.2110	-0.6868
3.0	0.6935	-0.0728	0.0178	0.0006	-0.0433	-0.3910
6.0	0.7023	-0.0746	0.0093	-0.0025	-0.0288	-0.2725
10.0	0.7035	-0.0746	0.0081	-0.0026	-0.0211	-0.2320

$\alpha = 0.80, \beta = \alpha/4$

l/h	a_r	a_i	b_r	b_i	e_r	e_i
0.2	0.2643	0.0486	0.0920	0.1963	-0.1757	-0.5355
0.5	0.3326	-0.0178	0.0955	0.1147	-0.3592	-0.6732
1.0	0.4188	-0.0732	0.0589	0.0381	-0.2724	-0.6386
3.0	0.4813	-0.0913	0.0095	-0.0001	-0.0742	-0.2774
6.0	0.4851	-0.0923	0.0060	-0.0019	-0.0326	-0.1711
10.0	0.4853	-0.0923	0.0058	-0.0020	-0.0257	-0.1470

$\alpha = 0.93$, $\beta = 0.22$

l/h	a_r	a_i	b_r	b_i	e_r	e_i
0.2	0.1943	0.0333	0.0724	0.1535	-0.2123	-0.5037
0.5	0.2554	-0.0231	0.0845	0.0896	-0.4062	-0.6419
1.0	0.3128	-0.0694	0.0451	0.0298	-0.2997	-0.5989
3.0	0.3603	-0.0839	0.0086	0.0013	-0.0735	-0.2122
6.0	0.3634	-0.0866	0.0065	0.0001	-0.0279	-0.1084
10.0	0.3625	-0.0841	0.0066	-0.0016	-0.0218	-0.0995

$\alpha = 0.99$, $\beta = \alpha/4$

l/h	a_r	a_i	b_r	b_i	e_r	e_i
0.2	0.1304	0.0171	0.0512	0.1060	-0.2420	-0.4938
0.5	0.1749	-0.0238	0.0635	0.0617	-0.4417	-0.6278
1.0	0.2108	-0.0556	0.0319	0.0214	-0.3138	-0.5714
3.0	0.2426	-0.0649	0.0081	0.0014	-0.0646	-0.1519
6.0	0.2434	-0.0651	0.0070	0.0007	-0.0173	-0.0620
10.0	0.2434	-0.0651	0.0070	0.0007	-0.0133	-0.0532

Appendix B

Asymptotic expression for the stress intensity factor due to in-plane residual stress in the layer

For a crack tip far away from the previous kink, the effect of the in-layer tensile residual stress σ_o is equivalent to a point force of magnitude $P = \sigma_o h$ per unit depth and a moment $M = \sigma_o h^2/2$ per unit depth acting as shown in Figure B1. When there is no elastic dissimilarity between the materials, $\alpha = \beta = 0$, the crack tip stress intensity factor is given by [9]

$$K_I^* \approx -(1/4)\sqrt{\frac{2}{\pi}}(h/\ell)^{3/2}\sigma_o\sqrt{h} \tag{B1}$$

$$K_{II}^* \approx -\sqrt{\frac{2}{\pi}}(h/\ell)^{1/2}\sigma_o\sqrt{h} \tag{B2}$$

When there is elastic dissimilarity, the complex interfacial stress intensity factor, $\mathbf{K}$, has a scaled magnitude and a shift in phase angle with respect to that of K_I^* and K_{II}^*, such that for large ℓ/h

$$\mathbf{K}h^{i\varepsilon} = \left(\frac{1-\alpha}{1-\beta^2}\right)^{1/2}(K_I^* + iK_{II}^*)e^{i\Omega} \tag{B3}$$

$\Omega(\alpha,\beta)$ is tabulated in [19].

Equations (B1), (B2) and (B3) may be combined to give an approximate expression for the complex quantity $e = e_R + ie_I$ in equation (5)

$$e_R = \frac{Re\mathbf{K}h^{i\varepsilon}}{\sigma_o\sqrt{h}} \approx -q\left[(1/4)(h/\ell)^{3/2}\cos\Omega - (h/\ell)^{1/2}\sin\Omega\right] \tag{B4}$$

$$e_I = \frac{Im\mathbf{K}h^{i\varepsilon}}{\sigma_o\sqrt{h}} \approx -q\left[(1/4)(h/\ell)^{3/2}\sin\Omega + (h/\ell)^{1/2}\cos\Omega\right] \tag{B5}$$

where $q = (\frac{2}{\pi})^{1/2}\left(\frac{1-\alpha}{1-\beta^2}\right)^{1/2}$.

We can use the asymptotic expressions (B4) and (B5) in order to deduce the critical length ℓ_c at kinking for large ℓ_c/h. Following the procedure discussed in

section 4.4, ℓ_c/h is a function of $\zeta = \sigma_o\sqrt{h}/\sqrt{\bar{E}_*\Gamma_I(\psi_c)}$, s/h, α and β. Typical results are shown in Figure B2: the asymptotic formulae compare favourably with the finite element results for $\ell/h > 5$.

List of figures

FIGURE

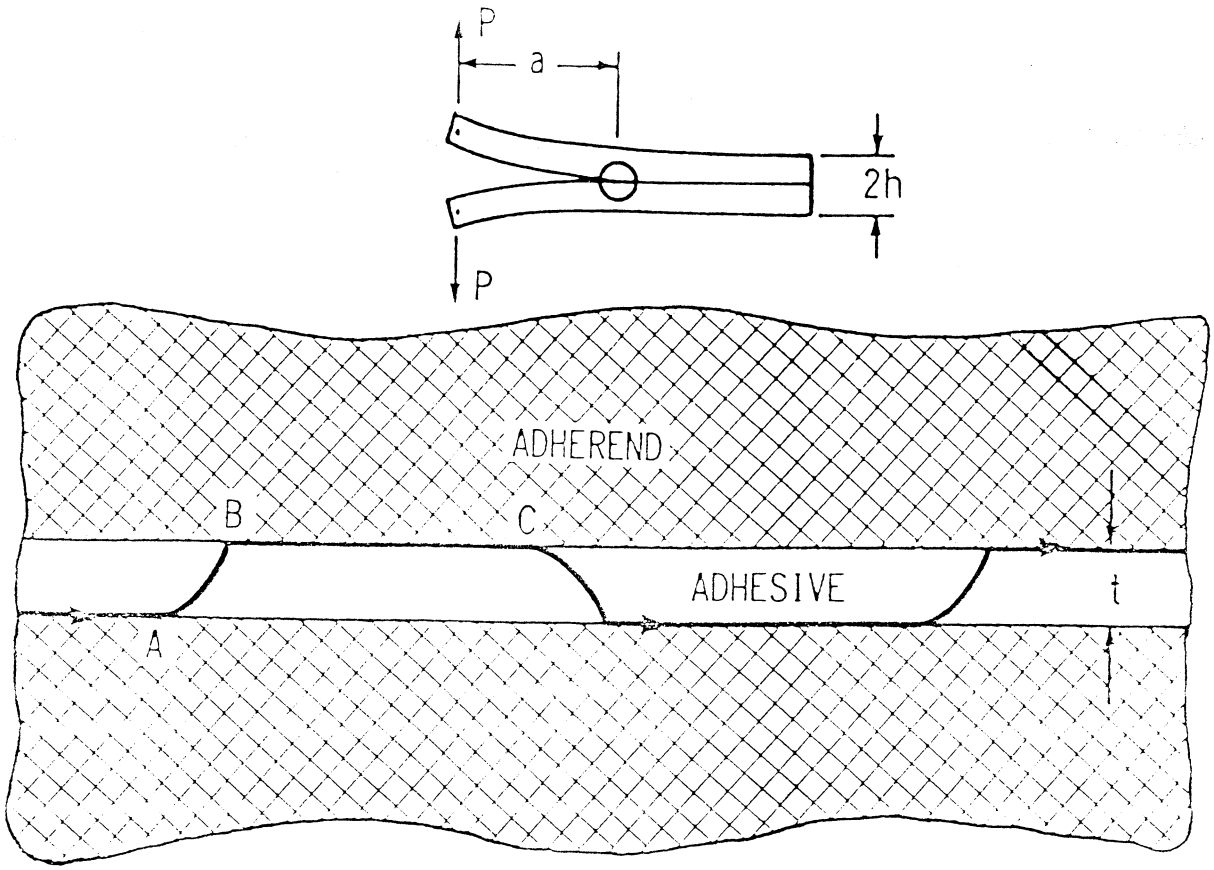

(a)

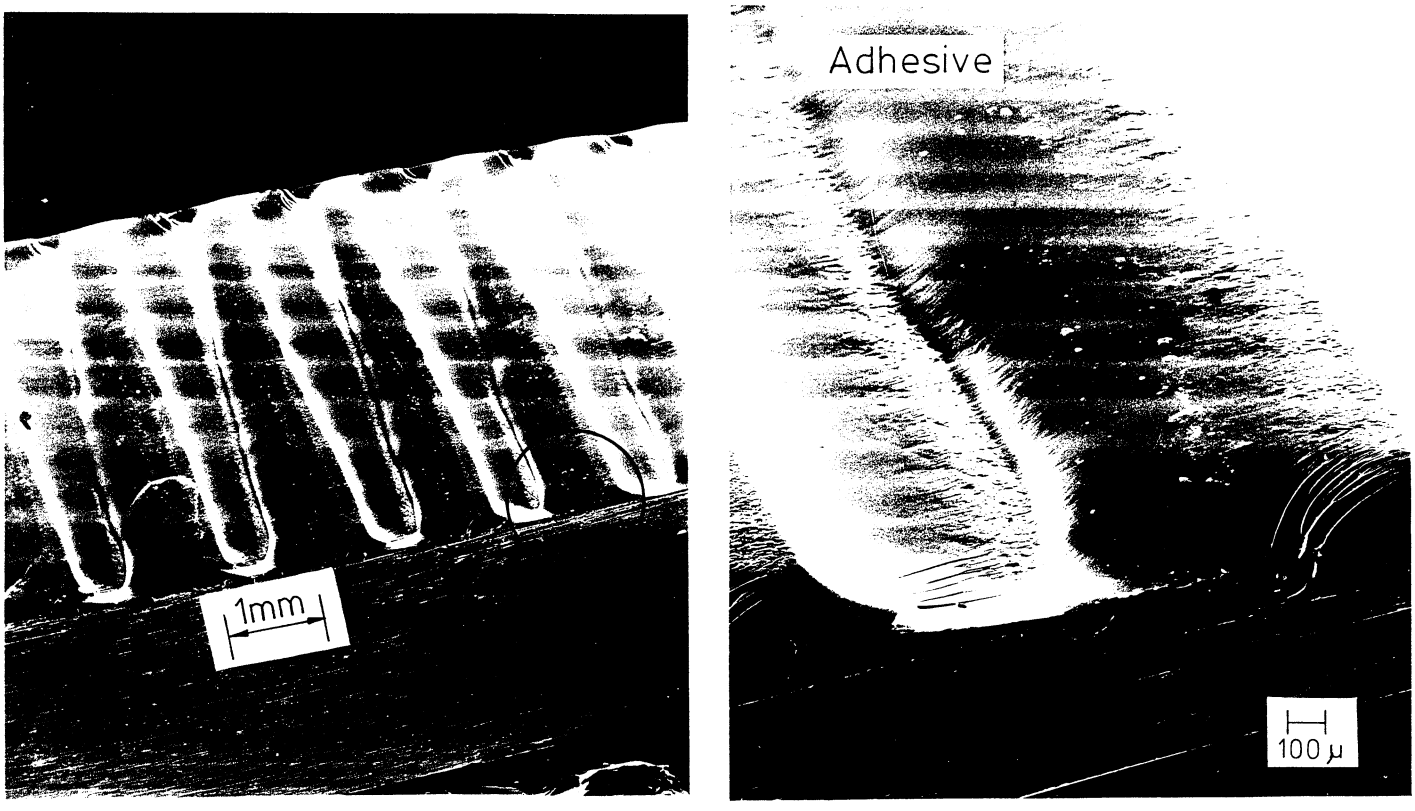

(b)

Figure 1: An alternating crack trajectory in a sandwich specimen. (a) The crack trajectory and (b) the fracture surface at two different magnifications. Taken from Chai [4].

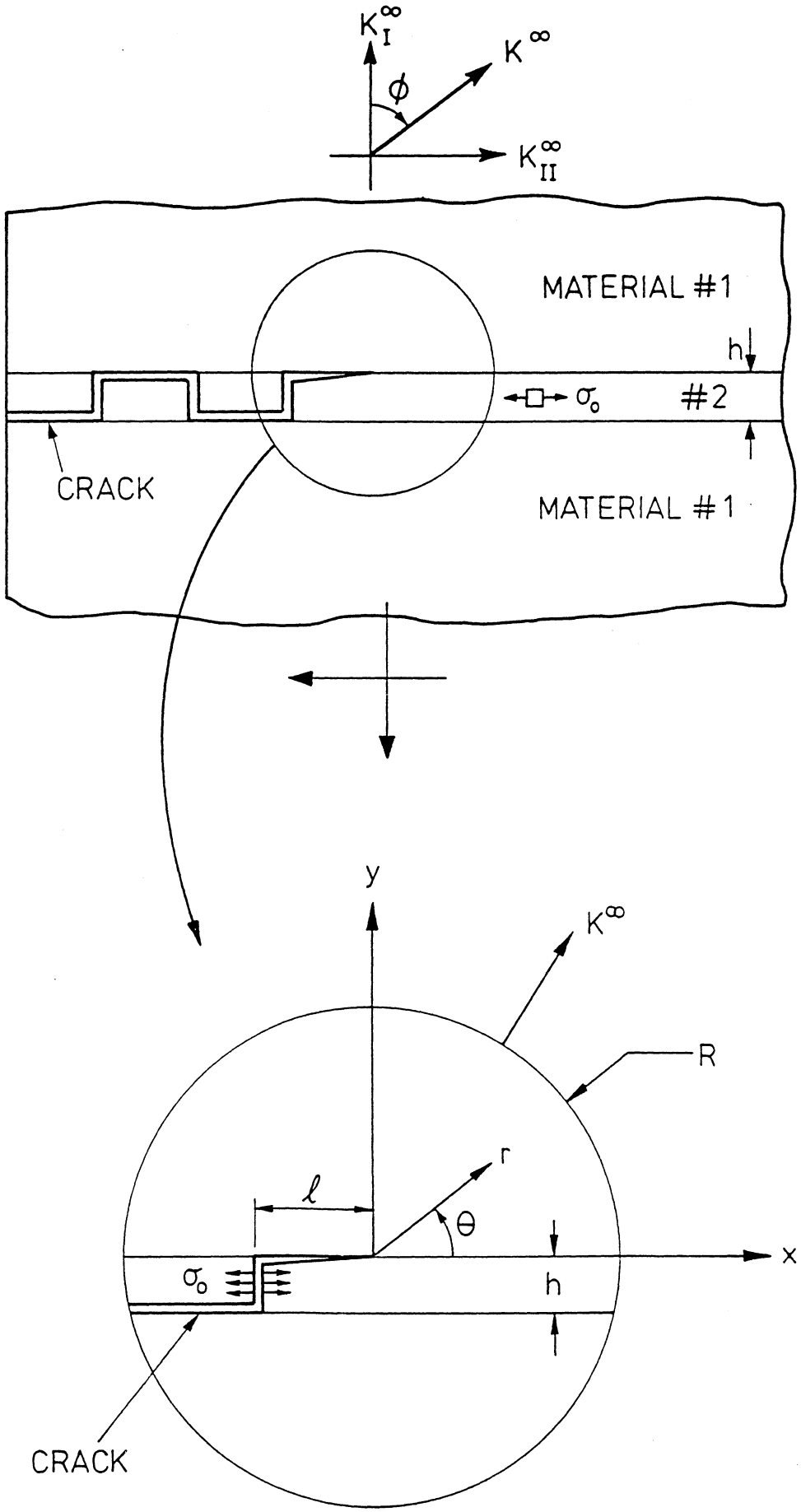

Figure 2: Idealised geometry for a wavy crack in an adhesive layer between two substrates.

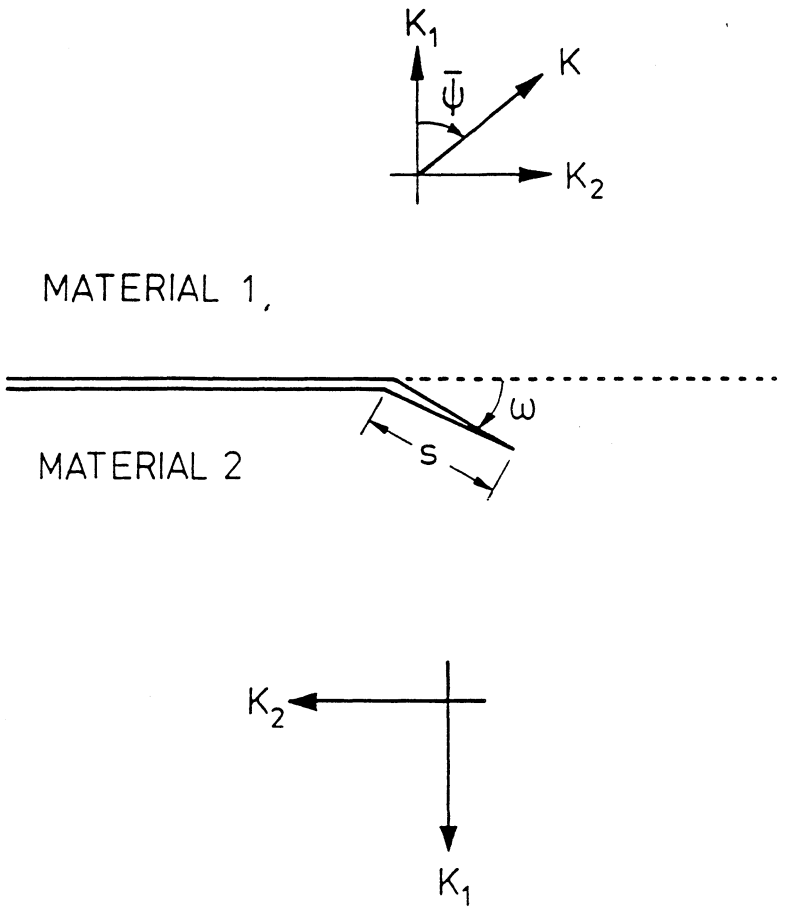

Figure 3: A crack kinking out of the interface.

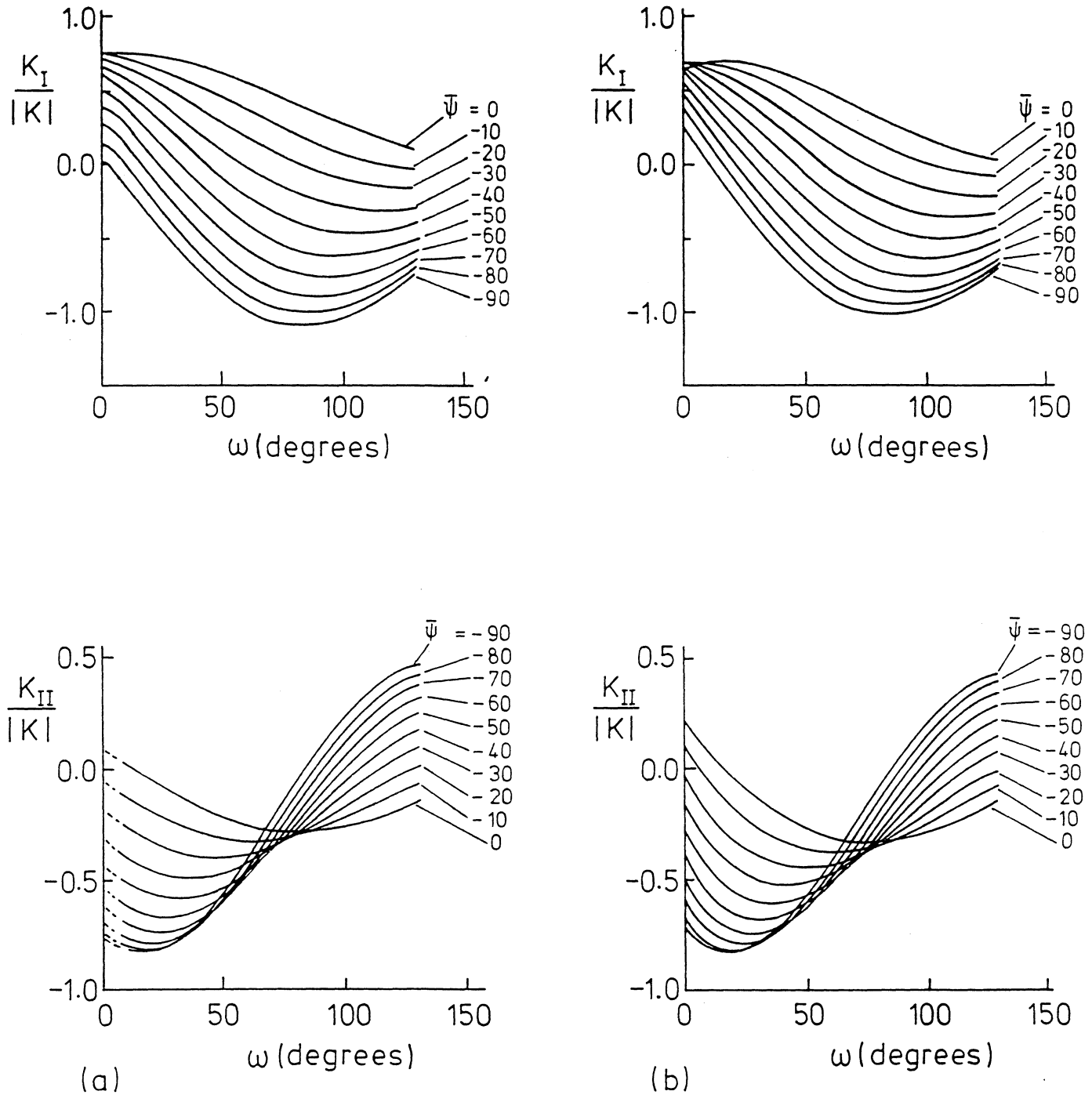

Figure 4: Effect of kink angle ω and phase angle $\bar{\psi} = \arctan[Im\mathbf{K}s^{i\epsilon}/Re\mathbf{K}s^{i\epsilon}]$ on the stress intensity factor at the tip of the kink. $\alpha = 0.8$, (a) $\beta = 0$ and (b) $\beta = 0.2$.

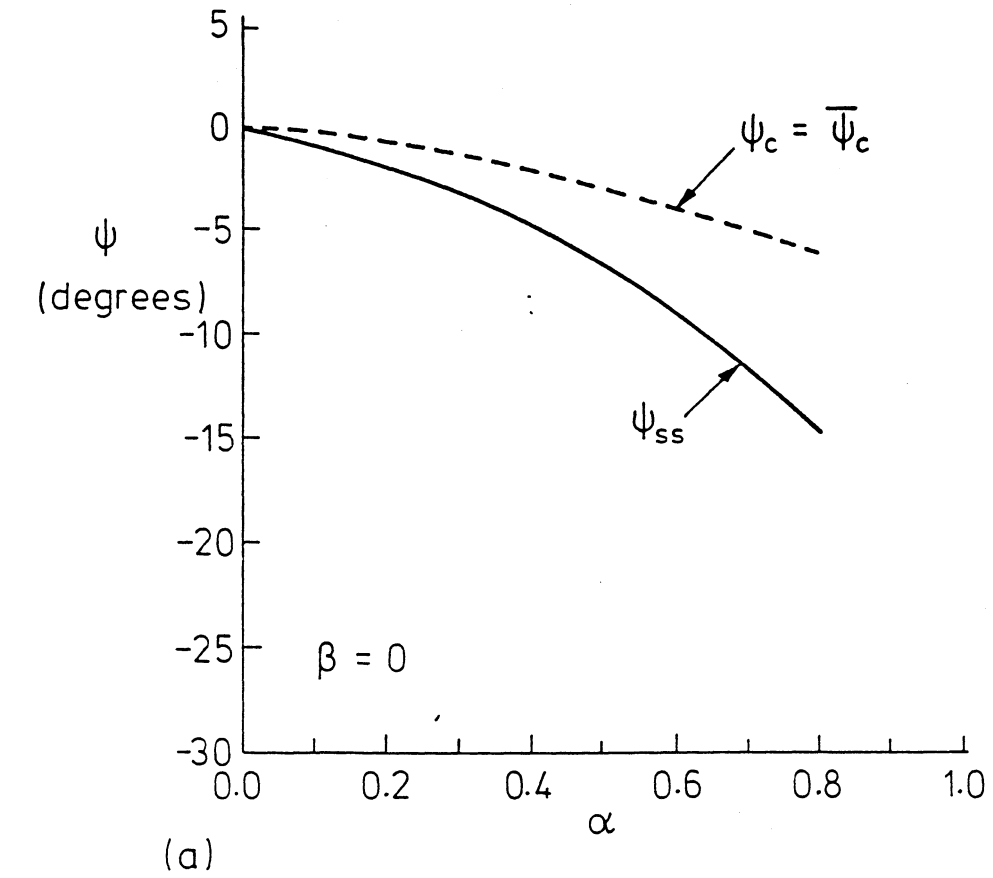

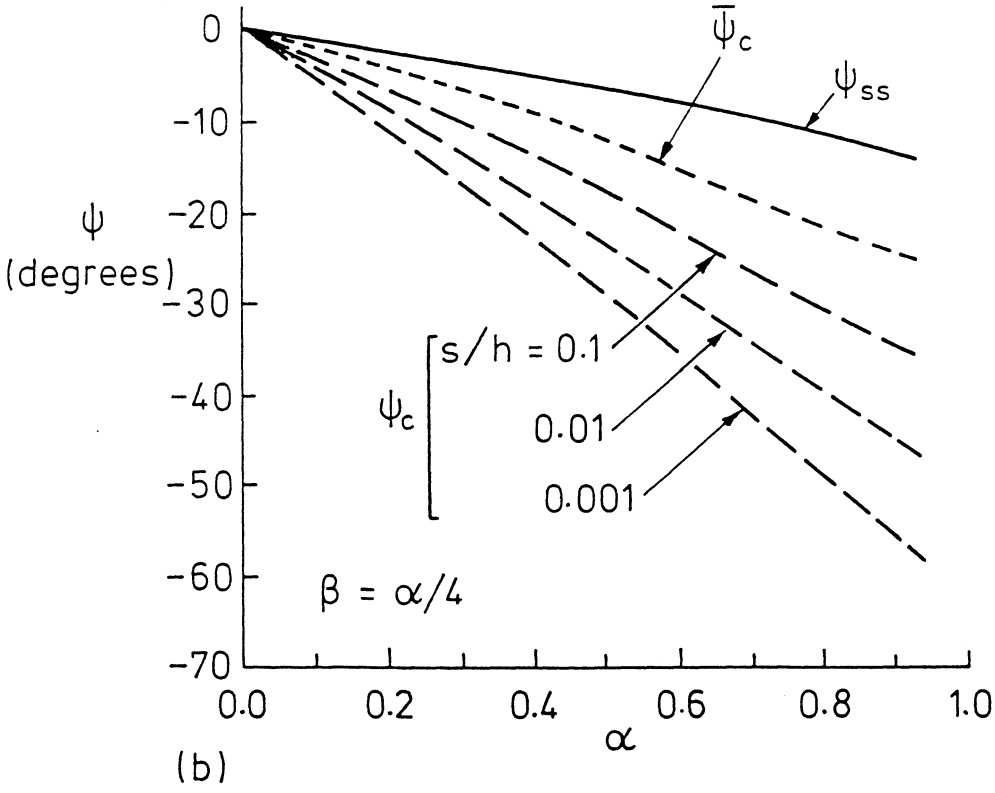

Figure 5: The dependence of critical phase angles ψ_c and $\bar{\psi}_c$ and steady state phase angle ψ_{ss} on elastic mismatch parameters α, β and relative flaw size s/h at the interface. (a) $\beta = 0$ and (b) $\beta = \alpha/4$.

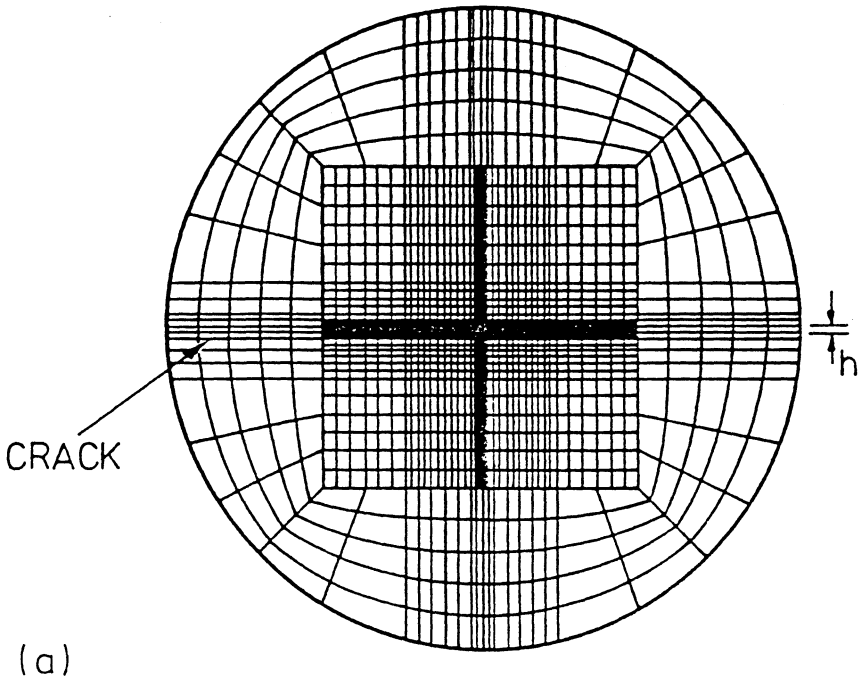

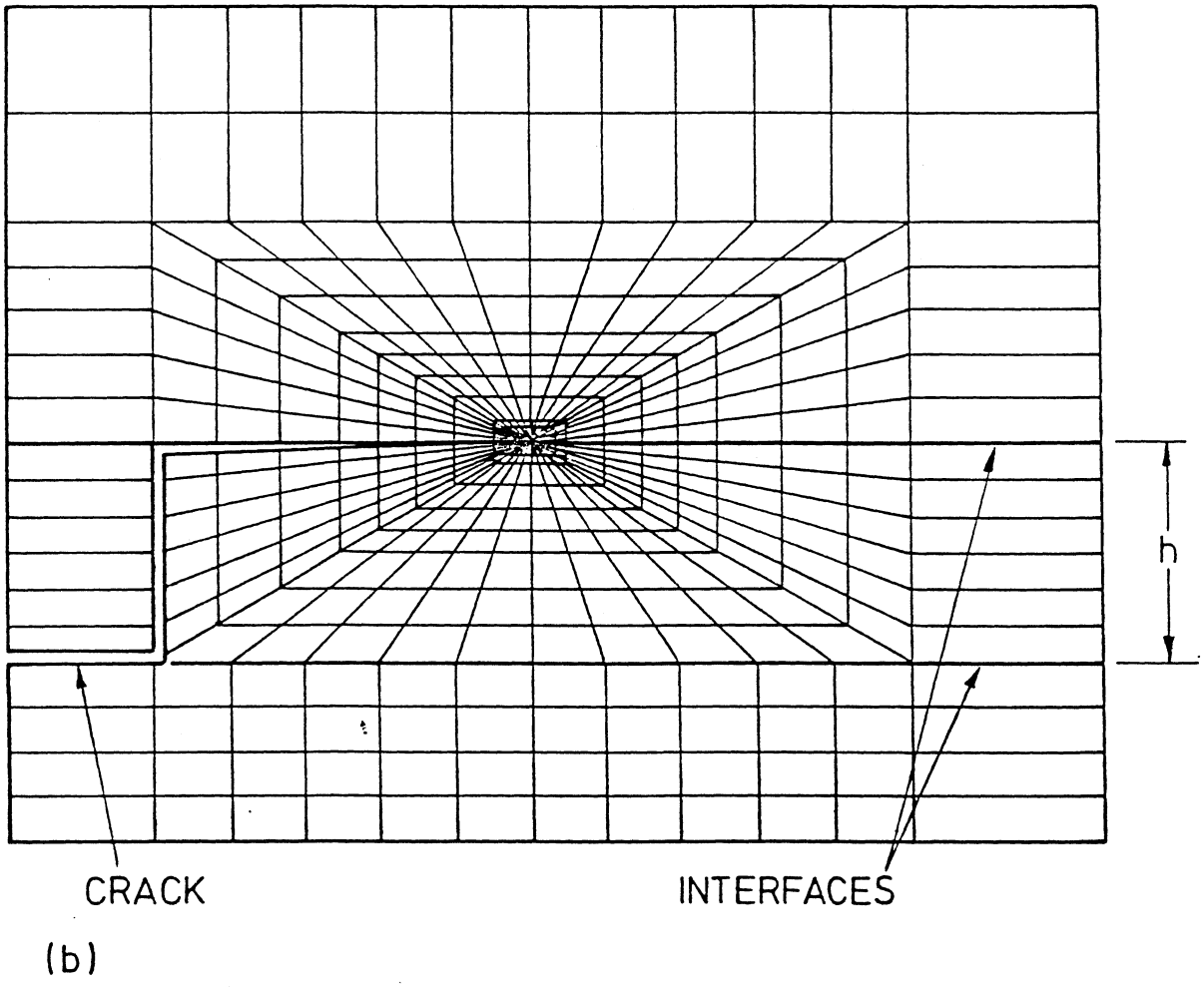

Figure 6: Finite element mesh. (a) The complete geometry, R/h = 50, total number of elements = 2460 and (b) near-tip region, crack tip element size = $0.03h$.

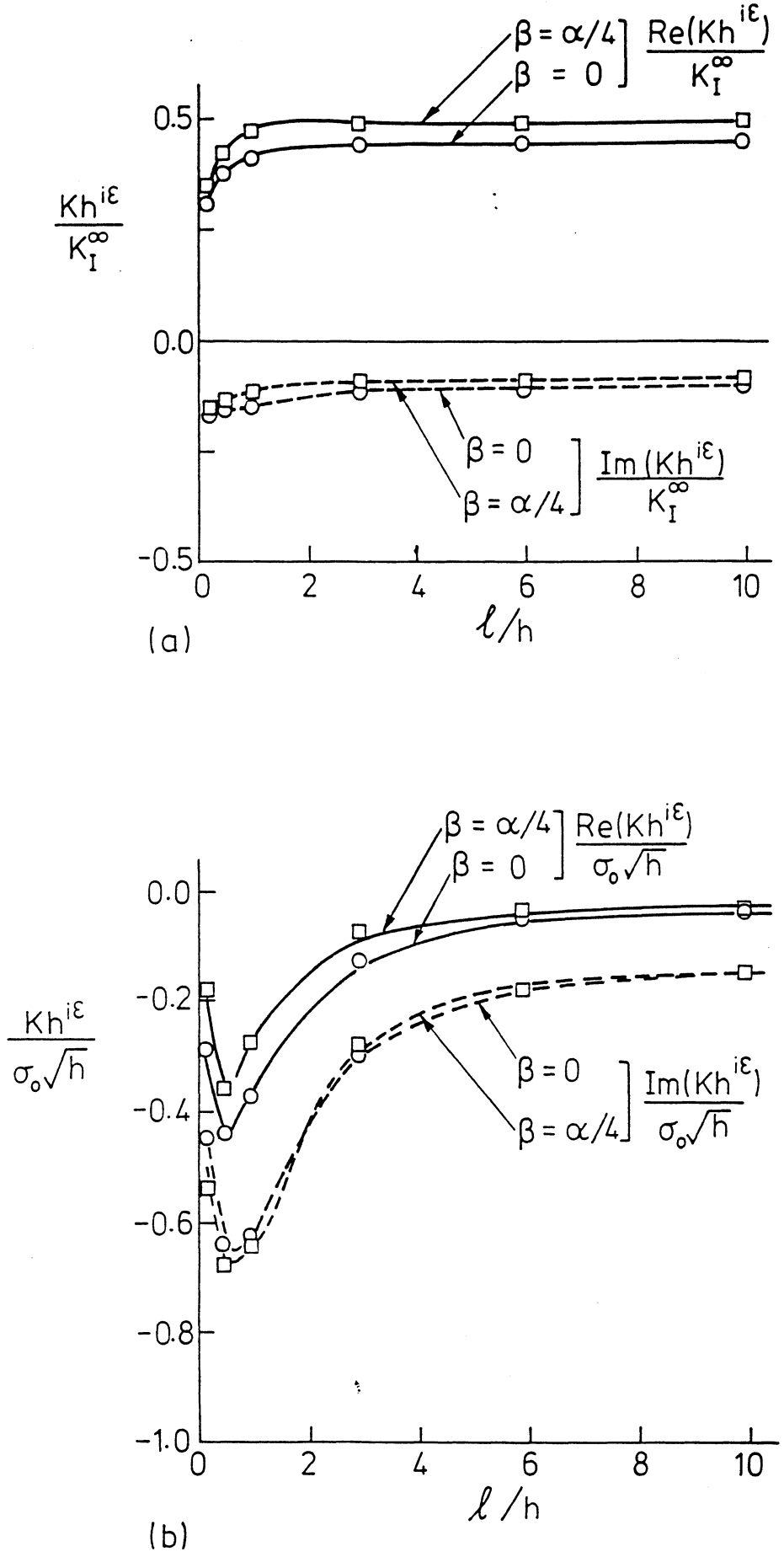

Figure 7: Non-dimensional stress intensity factor for the wavy crack due to (a) remote mode I load K_I^∞ and (b) in-plane tensile residual stress σ_o in the adhesive layer of thickness h. $\alpha = 0.8$.

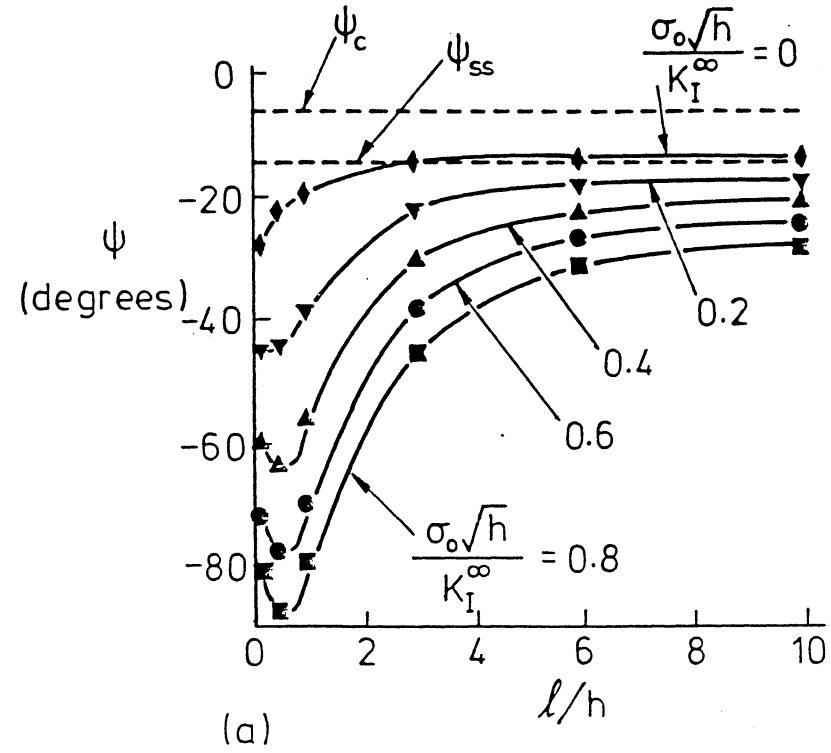

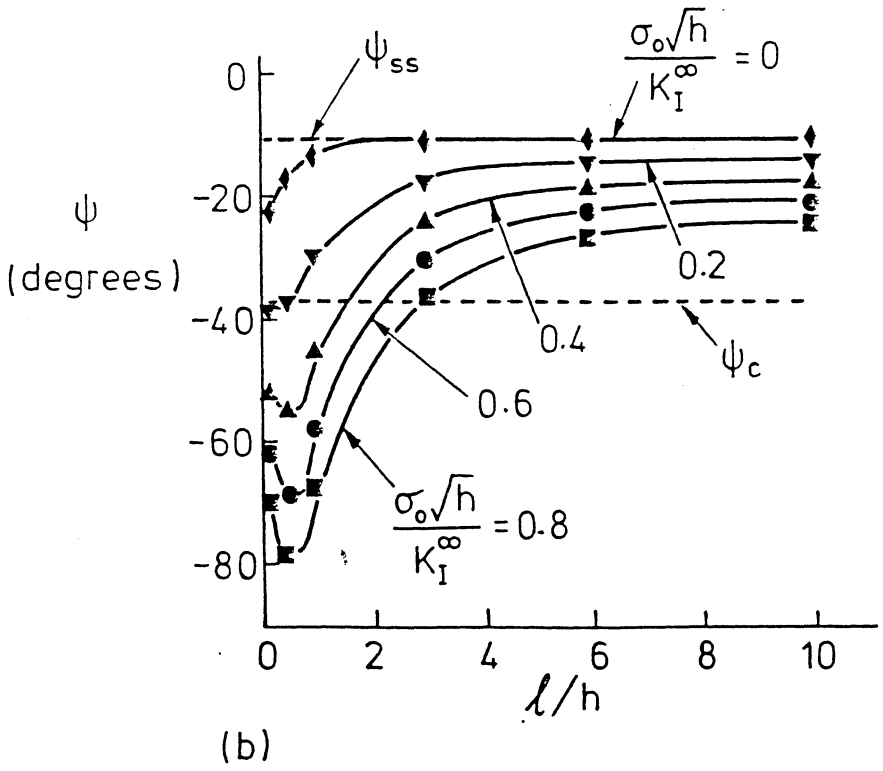

Figure 8: Effect of relative crack length ℓ/h and the non-dimensional residual stress $\sigma_o\sqrt{h}/K_I^\infty$ upon the interfacial phase angle $\psi = \arctan\left[\frac{Im(\mathbf{K}h^{ic})}{Re(\mathbf{K}h^{ic})}\right]$. $\alpha = 0.8$, ψ_c is for $s/h = 0.01$. (a) $\beta = 0$, and (b) $\beta = 0.2$.

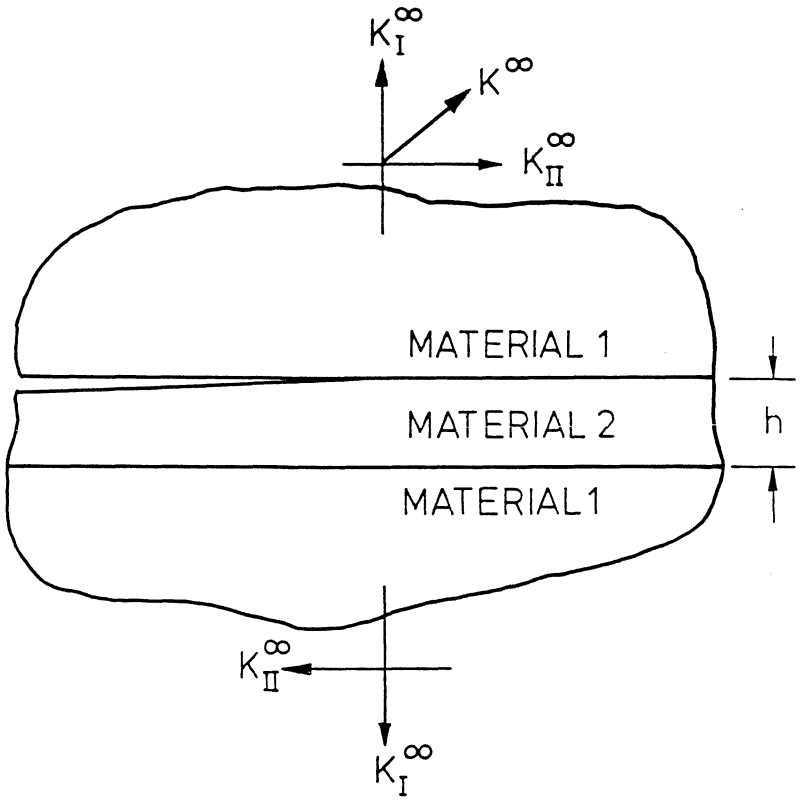

Figure 9: A semi-infinite interfacial crack in a sandwich specimen.

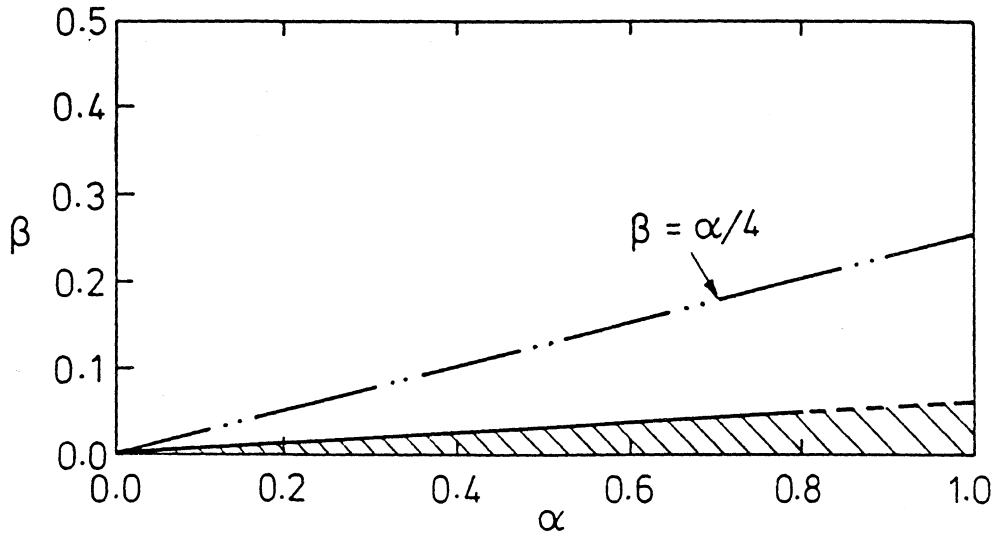

Figure 10: Region of possible alternating crack trajectory in α - β space, assuming a relative flaw size of $s/h = 0.01$. The hatched region is where the alternating crack trajectory is not expected.

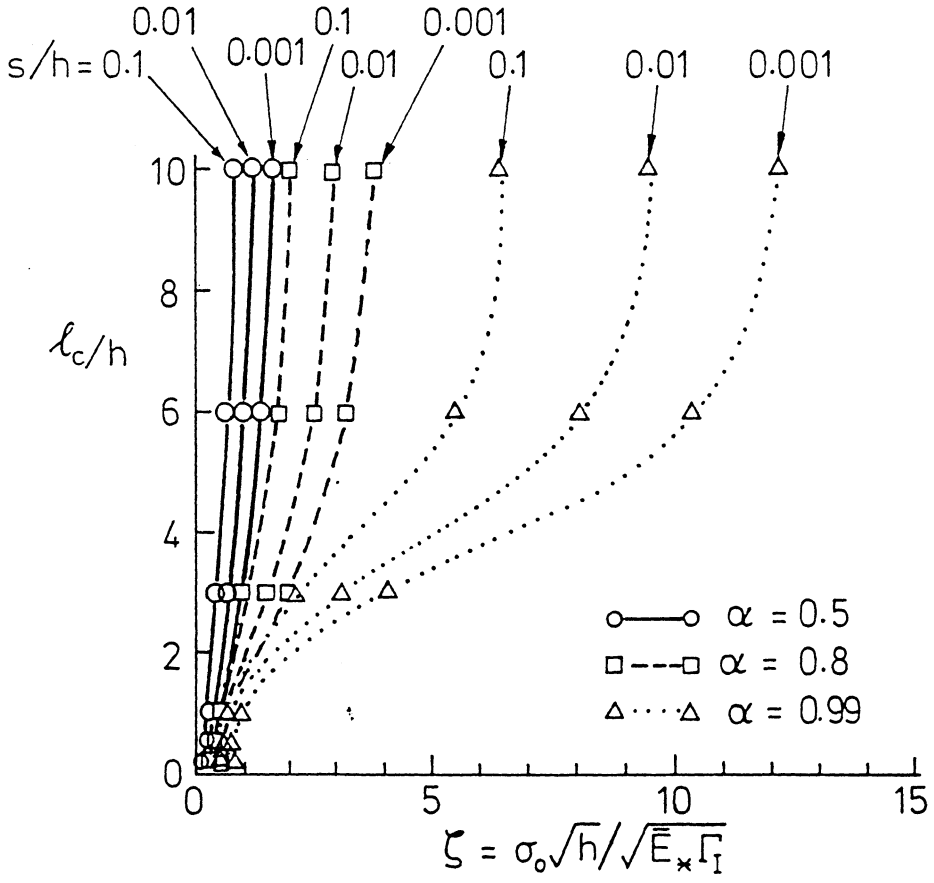

Figure 11: The dependence of the relative half wavelength of the alternating crack ℓ_c/h on the parameter $\zeta = \sigma_o\sqrt{h}/\sqrt{\bar{E}_*\Gamma_I}$.

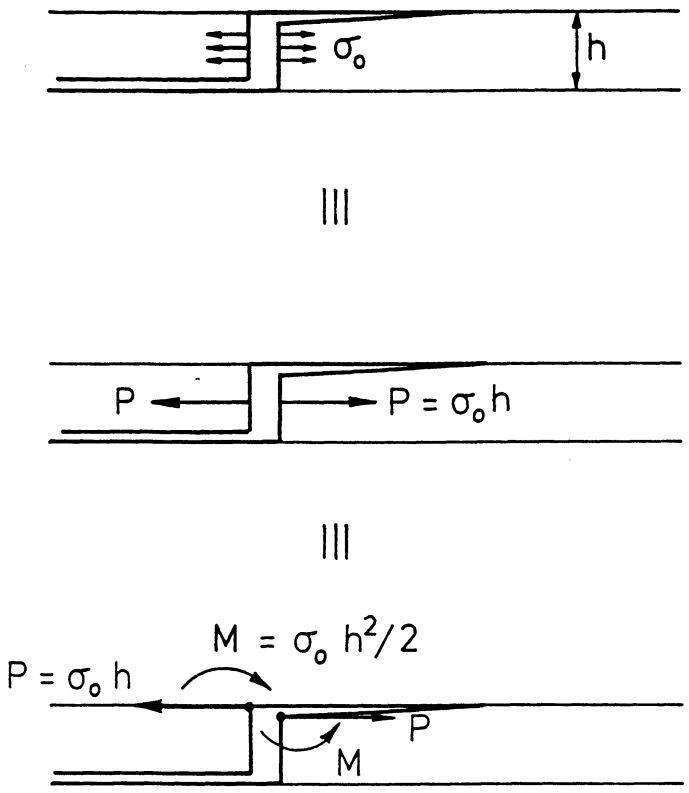

Figure B1: Equivalent loading condition for inplane tensile residual stress σ_o when the interfacial crack is long, $\ell/h >> 1$.

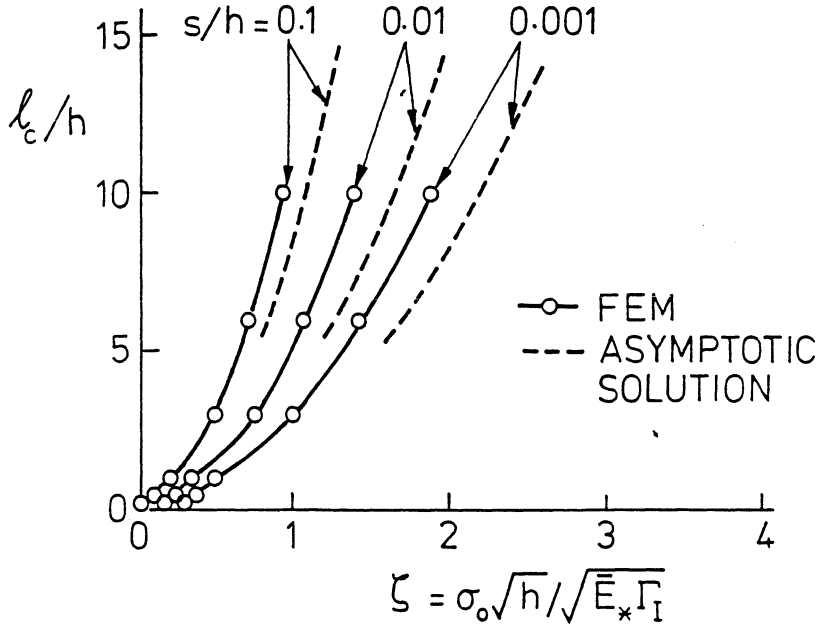

Figure B2: The dependence of the relative half wavelength of the alternating crack ℓ_c/h on the parameter $\zeta = \sigma_o\sqrt{h}/\sqrt{\bar{E}_*\Gamma_I}$. The asymptotic solution is included for $\alpha = 0.5$ and $\beta = \alpha/4$.